Contrib Mineral Petrol (2002) 144: 305–313
DOI 10.1007/s00410-002-0398-x

ORIGINAL PAPER

Theodore C. Labotka · Lawrence M. Anovitz
James G. Blencoe

Pore pressure during metamorphism of carbonate rock: effect of volumetric properties of H_2O–CO_2 mixtures

Received: 23 January 2002 / Accepted: 5 July 2002 / Published online: 29 August 2002

Abstract The molar volume of mixtures of CO_2 and H_2O is a strong function of the fluid composition. Both CO_2 and H_2O participate in the metamorphism of carbonate rocks, resulting in a change in the fluid composition during reaction. One of the effects of the change in composition is the increase in pore-fluid pressure with only small increases in extent of reaction, ξ. Pressure calculated from the volumetric properties of CO_2–H_2O mixtures at 400 °C increases greatly with small increases of ξ but drops at greater values because of the increase in pore volume as a result of ΔV_{solid}. The pore pressure increase at small values of ξ, though, readily exceeds the reported tensile strength of carbonate rocks, and the rock cannot sustain significant reaction without fracturing. The result of a small amount of reaction is a fractured rock with increased permeability, which promotes fluid transport.

Introduction

Fluids in many metamorphic rocks are essentially binary CO_2–H_2O mixtures. In some carbonate rocks, assemblages such as talc + calcite + dolomite indicate reactions that involve both CO_2 and H_2O. These reactions are accelerated by fluid flow, and reaction-produced fluid, in turn, affects the rates and patterns of fluid circulation. This feedback is influenced by the regional stress distribution, changes in the physical properties of the rock, and changes in the transport properties of the fluid (Norton and Dutrow 2001). For example, rock fracture caused by thermal expansion of water enhances host-rock permeability and promotes fluid flow (Domenico and Palciauskas 1979; Dutrow and Norton 1995). Changes in fluid pressure caused by fluid production during reaction can halt or even create back flow in circulating systems (Balashov and Yardley 1998; Dipple and Gerdes 1998).

CO_2 and H_2O have significantly different molar volumes at all metamorphic temperatures and pressures, and CO_2–H_2O mixtures are strongly non-ideal at $T \leq 500$ °C, $P \leq 100$ MPa (Labotka 1992). Seitz and Blencoe (1999) and Blencoe et al. (1999) measured the volumetric properties of CO_2–H_2O mixtures at 400 °C, $P \leq 100$ MPa. Those studies showed that the fluid density varies substantially with composition and that adding CO_2 to an H_2O-rich fluid can dramatically affect fluid properties, depending on the space occupied by the fluid. In a fixed volume, mixing results in increased fluid pressure. The rock can fracture under the increased pressure. If the rock is open to fluid flow, the increased pressure can effectively halt infiltration-driven metamorphic reactions. Mixing also results in a marked decrease in fluid density, which can induce buoyant flow under a wide range in metamorphic temperature and pressure. In this paper, we discuss the contribution of the volumetric properties of CO_2–H_2O fluids to pore pressure in rocks that behave as closed systems and the consequent likelihood that fluid-composition-buffering mineral assemblages are preserved in carbonate rocks.

T.C. Labotka (✉)
Department of Geological Sciences,
University of Tennessee, Knoxville,
Tennessee 37996-1410, USA
E-mail: tlabotka@utk.edu

L.M. Anovitz · J.G. Blencoe
Chemical Sciences Division,
Oak Ridge National Laboratory,
Oak Ridge, Tennessee 37831-6110, USA

Editorial responsibility: T.L. Grove

Rock-dominated fluid–rock systems

The existence of low-variance, fluid-composition-buffering assemblages indicates a rock-dominated system. In that kind of system, the mass of fluid that reacted with the rock was insufficient to overcome the capacity of the rock to fix the fluid composition. There are numerous examples of low-variance assemblages in

carbonate rocks. The regionally metamorphosed Noonday Dolomite from the Panamint Mountains, California (Labotka et al. 2000), is an example (Fig. 1). The protolith contained quartz grains in a dolomite matrix. Upon metamorphism, quartz and dolomite reacted to form talc and calcite. All four minerals are found together. Many other well-documented examples have been summarized by Rice and Ferry (1982).

A useful measure of the extent of reaction among the minerals and fluid is ξ, defined as the change in the number moles of a participant i in the reaction, normalized by the stoichiometric coefficient: $\xi = (n_i - n_i^\circ)/\nu_i$. The value of ξ can be determined from the mode and can be used to calculate the change in fluid composition during reaction, $dx_{CO2}/d\xi$.

We consider the case in which the rock was closed to externally derived fluids, and the only fluid that reacted with the rock was in the pore space. The process that is described here is a change in the composition of the fluid, a change in solid volume, and a change in the number of moles of the fluid phase because of reaction between the pore fluid and the rock. As a consequence, the pore fluid pressure increase is sufficient to cause fracturing. The purpose of this paper is to explore the consequences of reaction in mixed-volatile systems on fluid pressure, all other things being equal. We shall not consider in this paper reactions that occur under a change in temperature nor the rates of reaction or fracturing. Our discussion is limited to isothermal changes in fluid pressure as a consequence of mixing because the volumetric properties of the mixtures were measured accurately at 400 °C.

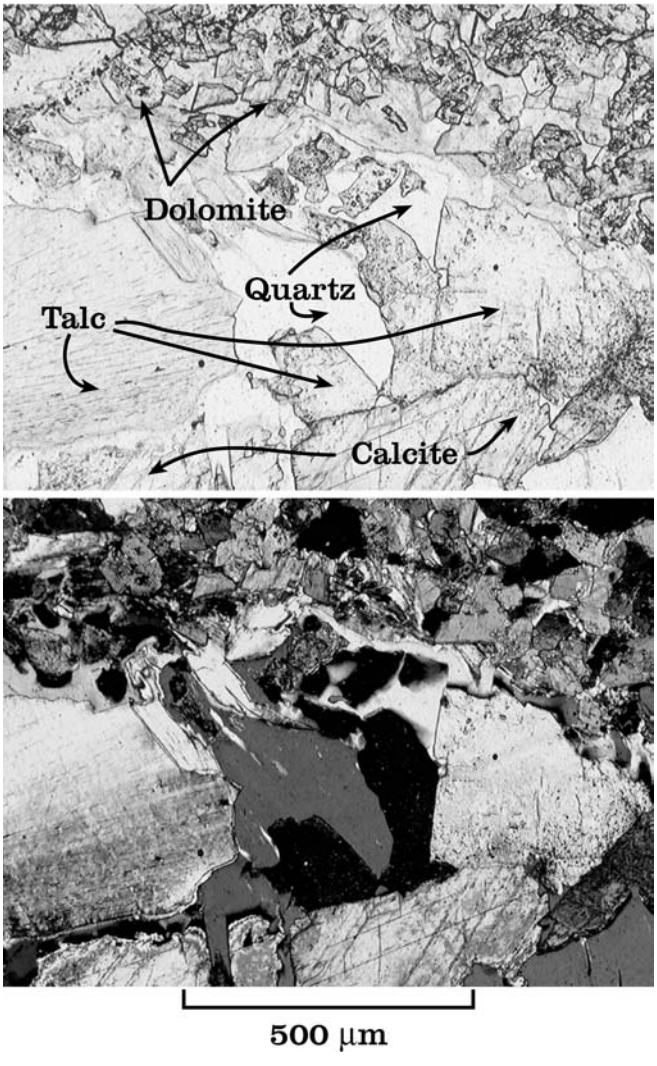

Fig. 1 Photomicrograph of metamorphosed Noonday Dolomite showing the low-variance assemblage dolomite + quartz + calcite + talc, which developed around detrital quartz grains. The upper micrograph is a plane-polarized view; the lower is in cross-polarized light

Volumetric properties of H_2O–CO_2 mixtures at 400 °C

Blencoe et al. (1999) developed a set of equations for the excess molar volume of mixtures of H_2O and CO_2 at 400 °C and 0–400 MPa with the use of volumetric data of Seitz and Blencoe (1999) and Sterner and Bodnar (1991). The expressions accurately predict the measured values for V^{ex} and permit calculation of activity-composition relations for the mixtures. Maximum values of V^{ex} (Fig. 2) are reached at 30 MPa for any given composition. The maximum occurs near the pressure of the critical isochore. At higher pressure, the mixtures behave more ideally. For any given pressure, V^{ex} is greatest in H_2O-rich compositions at pressure lower than 60 MPa and in CO_2-rich compositions at higher pressure. Other equations of state (Holloway 1977; Kerrick and Jacobs 1981; Duan et al. 1992) predict positive values of V^{ex}, but become increasingly inaccurate at temperature < 400 °C (Blencoe et al. 1999).

The pore reaction model

Isothermal changes in fluid pressure in rocks result from changes in volume and in composition during reaction. It is useful to consider a molar pressure, p, which is analogous to molar volume. For example, at 50 MPa and 400 °C, H_2O has a molar volume of 31.18 cm^3/mol; the analogous molar pressure is 50 MPa/mol at 400 °C and 31.18 cm^3. Changes in pressure at constant temperature are given by

$$dp = \left(\frac{\partial p}{\partial x}\right)_V dx + \left(\frac{\partial p}{\partial V}\right)_x dV \qquad (1)$$

where x is the fluid composition, x_{CO2}, and V is the fluid volume.

To calculate the pressure during reaction, two coefficients, representing the two partial derivatives, must be determined. The coefficients are the slopes of the curves in Fig. 3, which shows $p(x_{CO2})$ at constant volume and $p(V)$ at constant composition. As shown in Fig. 3a, the pressure of the H_2O–CO_2 mixture increases at constant

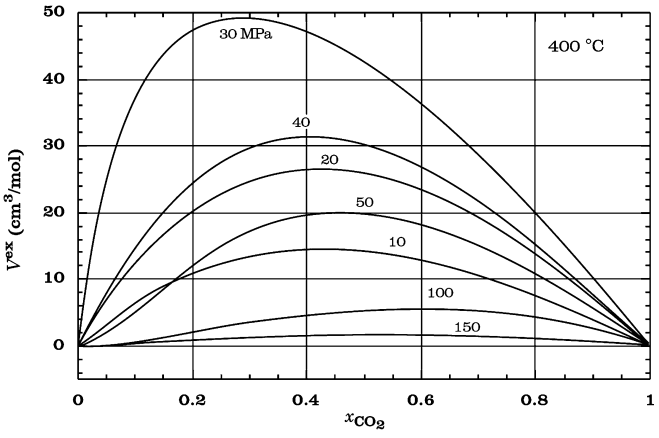

Fig. 2 Excess molar volume of CO_2–H_2O mixtures for selected pressures from 10 to 150 MPa

volume with an increase in x_{CO2}. This effect is greatest at small volumes, and pressure can exceed 400 MPa/mol with only a small fraction of CO_2 in volumes of 30 cm^3 or less. Figure 3b shows the increase in pressure at constant composition resulting from a decrease in volume. With the coefficients from the curves in Fig. 3, the change in pressure can be calculated from the change in volume and composition.

To examine the effects of mixed-volatile reactions on the pore pressure, we employ a simple model for the pore structure of a rock. In this model, the pore space can have any shape. As reaction proceeds, the volume of the pore increases as a result of the ΔV_{solid}, reactant pore fluid components are incorporated in the product minerals, and product fluid components are added to the pore fluid. No fluid from any external source is added.

The rock is considered to have negligible compressibility because of its extremely small contribution to the ΔV_{solid}. Compressibility could be incorporated if necessary. The pressure in the pore generally increases, and in calculation of mineral equilibria, the pressure on the product and reactant minerals is that of the pore fluid. The pore-fluid pressure before reaction is the same as the confining pressure, but generally increases as a result of reaction. The initial pore fluid composition is taken to be H_2O, and temperature is raised instantaneously to 400 °C, at which reaction begins.

The calc-silicate equilibria considered are

$$3\ \text{dolomite} + 4\ \text{quartz} + H_2O = \text{talc} + 3\ \text{calcite} + 3\ CO_2, \quad (2)$$

$$3\ \text{calcite} + \text{tremolite} + 2\ \text{quartz} = 5\ \text{diopside} + H_2O + 3\ CO_2, \quad (3)$$

$$5\ \text{dolomite} + 8\ \text{quartz} + H_2O = \text{tremolite} + 3\ \text{calcite} + 7CO_2 \quad (4)$$

$$\text{calcite} + \text{quartz} = \text{wollastonite} + CO_2\ \text{and}, \quad (5)$$

$$3\ \text{anorthite} + \text{calcite} + H_2O = 2\ \text{clinozoisite} + CO_2. \quad (6)$$

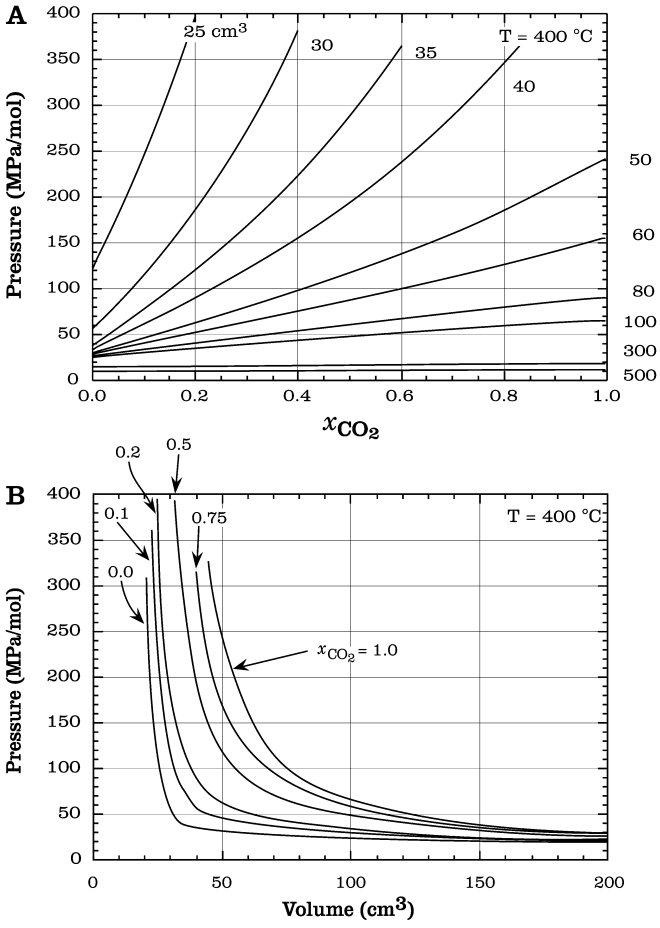

Fig. 3A, B Coefficients for the expansion of dp as a function of volume and composition are determined from the slopes of these curves. These are used to calculate the pressure per mole of fluid in pores in rock during metamorphism. **A** Isovolume curves showing the change in pressure with composition, $(\frac{\partial p}{\partial x_{CO_2}})_V$. **B** Curves of constant composition showing the change in pressure with volume, $(\frac{\partial p}{\partial V})_{xCO_2}$

These equilibria are shown on an isothermal p-x section in Fig. 4. Values of $f^{\circ}_{CO_2}$ were taken from Span and Wagner (1996), and the values of $f^{\circ}_{H_2O}$ are those of Wagner and Pruss (1993). The activity–composition relations are those of Blencoe et al. (1999). The mineral thermodynamic data used in the calculation of Fig. 4 are those of Holland and Powell (1990), which is admittedly a minor inconsistency because they used the EOS of Kerrick and Jacobs (1981) to derive some of the mineral data. The loss of self-consistency is unavoidable because other self-consistent databases also use the Kerrick and Jacobs EOS for the fluid phase.

The difference between the use of Blencoe et al. (1999) and Kerrick and Jacobs (1981) on the calculated equilibria is shown for the calculated pressure of reaction (2) in the inset in Fig. 4. For H_2O-rich compositions, the MRK model of Kerrick and Jacobs (1981) predicts an equilibrium pressure more than 100 MPa greater than that derived from Blencoe et al. (1999) equations. The difference is small for CO_2-rich compositions, but can

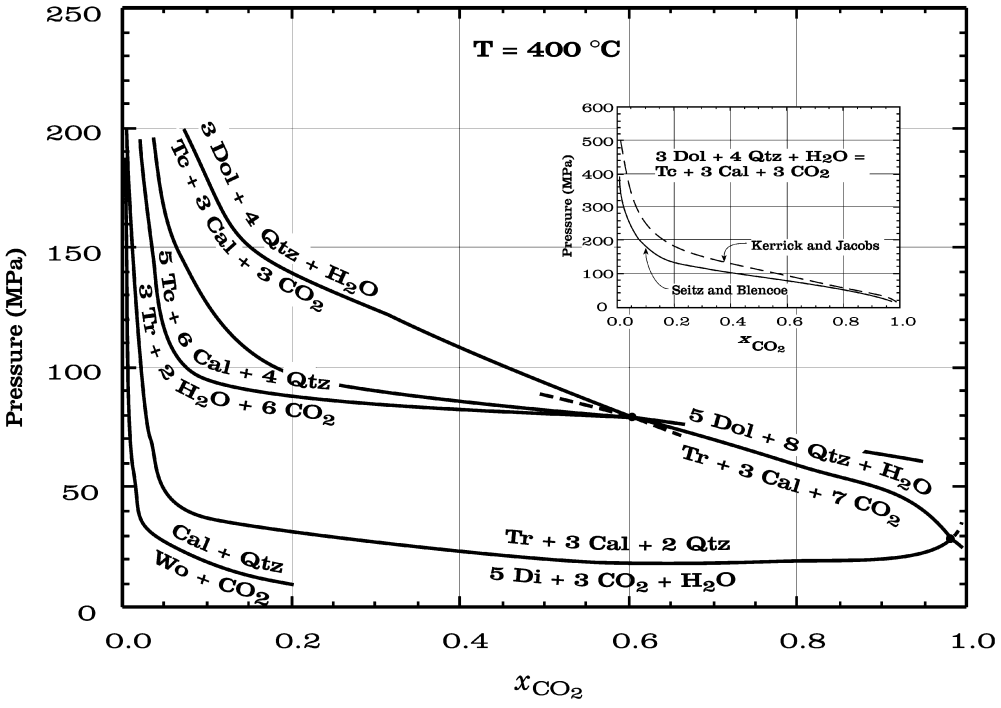

Fig. 4 Pressure-composition diagram at $T = 400$ °C for several mixed-volatile reactions. The *inset* shows the difference between the models of Kerrick and Jacobs (1981) and Seitz and Blencoe (1999) for the activities of CO_2–H_2O mixtures on the talc-forming reaction

have a significant effect on calculated equilibria for H_2O-rich, low-temperature conditions.

The rock compositions used in the model are similar to samples from the Panamint Mountains, with a dolomite/quartz mass ratio of 9 (Labotka and Souza 2002), and from the Notch Peak aureole, with a calcite/quartz mass ratio of 7/3 (Labotka et al. 1988). In most cases, the extent of reaction in the model is small and never exceeds the buffer capacity, so the rock composition only affects the extensive properties, in particular, the value of ξ.

The starting porosity assumed in the model has a considerable effect on the results. For most of the discussion, the assumed initial porosity is 0.1%. Calculations are performed for several confining pressures ranging from 25 to 200 MPa. For each pressure, the reference volume of rock chosen to monitor the change in pore pressure is the volume sufficient to contain 1 mol of H_2O within the 0.1% pore volume. The reference volume changes because the molar volume of water depends on pressure (Fig. 3); at low pressure, a larger volume of rock is needed to hold 1 mol in the pore space than at high pressure. Reference volumes range from 0.2 to 0.3 m^3 for the pressure range chosen. To remove the variable reference volume, all calculated extents of reaction within the volume are normalized to a weight basis: mol/kg rock. The model parameters for all the calculations are given in Table 1.

We use the equilibrium 3 dolomite + 4 quartz + H_2O = talc + 3 calcite + 3 CO_2 to describe the calculation of the pore pressure and volume. As reaction proceeds, the volume of the pore space increases because of the ΔV_{solid}, the fluid in the pore becomes CO_2-rich because of the production of 3 mol of CO_2 for every mol of H_2O consumed, and the pressure in the pore increases because of the change in fluid composition and the net increase in the number of moles of fluid in the pore. Reaction proceeds until one of the reactants is consumed, or until the equilibrium fluid composition is reached. The equilibrium fluid composition at 400 °C depends on the fluid pressure, which changes from the confining pressure as reaction proceeds.

The pore pressure is calculated numerically by incrementing ξ, calculating the fluid composition, and calculating the ΔV_{solid}. The molar pressure of the new pore fluid is determined from Eq. (1) with the use of the coefficients determined from the slopes of the curves in Fig. 3. The pore pressure is determined from that calculated value times the number of moles of fluid in the pore.

The resulting pressure in the pore volume as a function of the extent of reaction is shown in Fig. 5. The pressures were calculated at confining pressures of 25–200 MPa. The extents of reaction for which the pressures were calculated, in general $\xi < 0.010$, are less than the buffer capacity of the model rock, 0.003–0.015 mol/kg at 25–200 MPa (corresponding to the amount of H_2O initially in the pore volume). We terminated the calculations at values of ξ where the pressure increase far exceeded the equilibrium values. The characteristics of the model are an increase in pressure with increase in ξ to a maximum value, followed by a pressure decrease. The maximum in the curve is located where the increase in pressure caused by reaction and by change in fluid composition is matched by the increase in volume caused by the negative ΔV_{solid}. The maximum in pressure always occurs at extents greater than the equilibrium value for the isothermal system. The equilibrium values are indicated on the right side of Fig. 5; these are

Table 1 Parameters used in model calculations with examples values at 50 MPa. Reactions are:
2 3 dolomite +4 quartz + H_2O; = talc + 3 calcite + 3 CO_2,
3 3 calcite + tremolite + 2 quartz = 5 diopside + H_2O + 3 CO_2,
4 5 dolomite + 8 quartz + H_2O = tremolite + 3 calcite + 7CO_2
5 calcite + quartz = wollastonite + CO_2
6 3 anorthite + calcite + H_2O = 2 clinozoisite + CO_2

Reaction	2	3	4	5	6
Starting dolomite (g/kg)	900		900		
Starting quartz	100	200	100	300	
Starting calcite		700		700	900
Starting tremolite		100			
Starting anorthite					100
ΔV_{solid} (cm^3/mol)	–36.76	–98.51	–119.52	–19.692	–66.46
V_{rock} (cm^3/mol)	351.78	367.65	351.78	371.978	368.3
Porosity (fraction)	0.001	0.001	0.001	0.001	0.001
V fluid	0.352	0.368	0.352	0.372	0.368
Confining pressure (MPa)	50	50	50	50	50
v_{H2O} (cm^3/mol)	31.18	31.18	31.18	31.18	31.18
n^0 H_2O (mol/kg rock)	0.011	0.012	0.011	0.012	0.012

the values of x_{CO2} at the indicated pressure and are related to ξ by the relation

$$x_{CO_2} = \frac{v_{CO_2}\xi}{n^0_{H_2O} + (v_{CO_2} + v_{H_2O})\xi}.$$

in which $n^0_{H_2O}$ is the initial amount of H_2O in the pore space and v_i is the stoichiometric coefficient of i.

Pore pressure and rock strength

This analysis shows that there is a substantial increase in pressure with only a small amount of reaction. For example, with a confining pressure of 50 MPa, pore pressure increases to 140 MPa at a value of $\xi = 9\times10^{-4}$ mol/kg when the equilibrium value of $x_{CO2} = 0.196$ is attained. For all confining pressures considered, the pore pressure increases by more than 50 MPa. Rocks certainly do not behave as rigid solids, but deform in response to the increase in stress. If the carbonate rocks behave as elastic solids under the considered conditions, the increased pore pressure causes expansion of the pore and leads to failure. The result is a fracture that grows during reaction not only by the causes considered in the model, but also by propagation during brittle failure.

The principles of the propagation of fractures in rock because of increased pore pressure was described by Jaeger and Cook (1976), Atkinson (1987), Lockner (1995), and many others. The criterion for failure from the Griffith theory for a crack with internal pressure is

$$\sigma_3 - p = -T_0 \qquad ()$$

in which the effective stress is the difference between the normal stress and the pore pressure p. T_0 is the tensile strength of the rock. The value of T_0 depends on several factors, including temperature, fluid composition, and rock anisotropy. Measured values of T_0 for all rock types rarely exceed 50 MPa; limestone and marble have average measured values of ~15 MPa (Lockner 1995). We chose the maximum observed value of 50 MPa for T_0 to illustrate the relation between reaction and fracture. Smaller values of T_0 result in failure at smaller values of ξ.

With a confining pressure of 50 MPa as an example, the talc-forming reaction proceeds until the pore pressure is 100 MPa (Fig. 5, enlarged in Fig. 6a). Once pressure reaches 100 MPa, which occurs at a value of $\xi = 4\times10^{-4}$ kg^{-1}, the rock fractures. If rock failure is catastrophic, then the fluid pressure drops to lithostatic, hydrostatic, or even lower pressure, and the rock may become open to fluid flow. Figure 6a shows the case for which pressure in the opening fracture returns to the lithostatic value. The volume of the fracture is determined by the molar volume of the H_2O–CO_2 mixture at 400 °C and 50 MPa. As the assemblage continues to react, the pressure again increases until fracturing recurs. Once the fluid composition and pressure reach the equilibrium value, reaction stops. If the cracks continue to open until the fluid pressure relaxes to the lithostatic value, the fluid composition follows the equilibrium curve. The pore volume increase during reaction and fracture, shown in Fig. 6b as the fractional porosity, ϕ, is determined by the molar volume of the H_2O–CO_2 mixture and the number of moles of fluid at the pressure given in Fig. 6a. The porosity increases by virtue of the ΔV_{solid}, the opening of the fractures, and by reaction along the equilibrium curve. Porosity increases primarily by crack growth during fracture and during reaction along the equilibrium curve. Once the fluid reaches lithostatic pressure, its composition is $x_{CO2} = 0.827$, and the model porosity is 0.64%: a sixfold increase from the starting value.

If crack growth instead comes about by subcritical crack growth or by stress corrosion, then the pore pressure remains at a threshold value. Continued reaction results in increased crack volume as the crack grows. This is illustrated in Fig. 7, in which the threshold value is assumed to be 50 MPa to facilitate comparison with the previous case. Reaction proceeds at 100 MPa until the equilibrium pressure is reached at $\xi = 2.4\times10^{-3}$

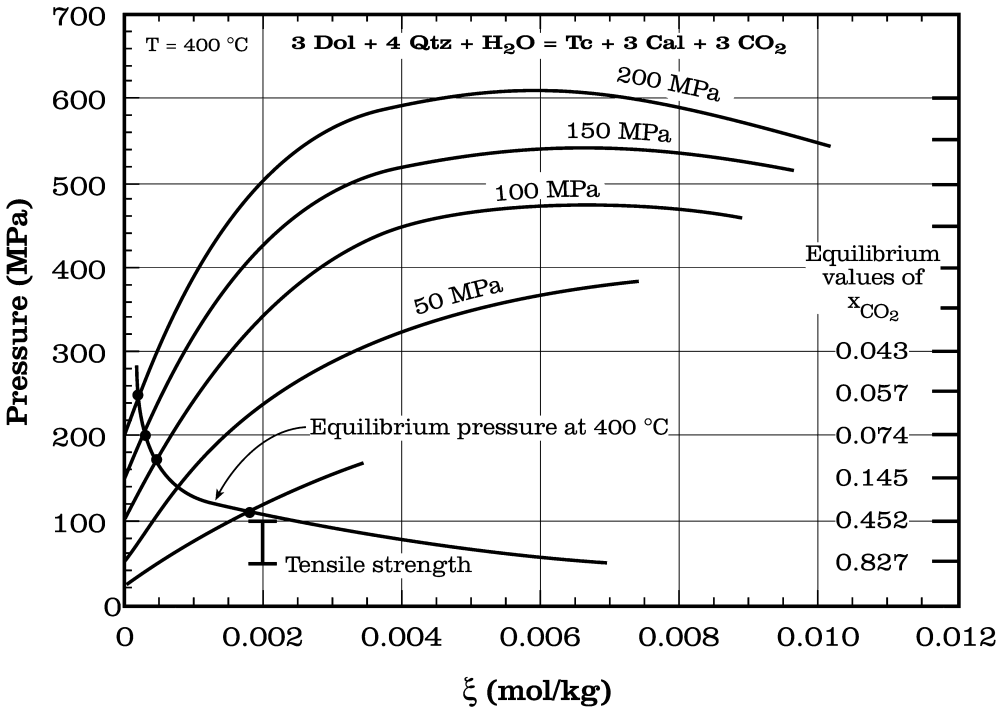

Fig. 5 Increase in pore pressure resulting from the talc-forming reaction. The negative-sloped curve is the equilibrium pressure at 400 °C. The corresponding fluid composition is shown on the right. The 50-MPa bar shows the tensile strength used in subsequent figures to show the growth of cracks during the reaction

kg^{-1}. If the crack continues to grow until the pore pressure relaxes to the lithostatic value, reaction proceeds along the equilibrium curve until $x_{CO2} = 0.827$ at $\xi = 6.8 \times 10^{-3}$ kg^{-1}. Figure 7b shows the growth in pore space with reaction and crack growth. The pore volume increases slightly during reaction until a pressure of 100 MPa is reached. The volume increases along the 100 MPa isobar by crack growth until the equilibrium value of $x_{CO2} = 0.45$, where continued reaction can only occur if crack growth continues until lithostatic pressure is attained. Pore volume increases from 0.1 to 0.64%. In each case (Figs. 6 and 7), the end result is the same: the final values of ξ, x_{CO2}, and ϕ are identical for each.

Discussion

The results shown for the example talc-forming reaction are readily extended to other initial conditions and to other reactions. The results scale geometrically by changing the initial porosity. For example, if the initial porosity is 1.0% instead of 0.1%, the final fracture volume, 6.4%, is a factor of 10 greater than that in the example. The final fluid composition remains the equilibrium composition, but the amount of reaction required to reach the final composition is 10 times greater than in the example, 0.068 mol/kg. The buffer capacity of the rock–fluid system is never exceeded.

The failure condition of $T_0 = 50$ MPa ascribes great strength to carbonate rock, especially for a temperature of 400 °C; most measured values are lower (Lockner 1995). The effect of a lower tensile strength is failure at smaller pore pressures and smaller extents of reaction. The maximum pore pressure such a rock would achieve would be accordingly lower, but the end product of the modeled processes of either Fig. 6 or 7 would be the same equilibrium value of ξ, x_{CO2}, and ϕ. The difference is that a greater number of fracture episodes would have occurred.

Confining pressure affects both the critical stress needed to propagate fractures and the equilibrium value of x_{CO2}. With increased confining pressure, the amount of reaction required to reach equilibrium is reduced, as can be seen in Fig. 5. The extent of reaction and the final pore volume are determined by the equilibrium value of x_{CO2} at the confining pressure. Because the H_2O–CO_2 fluid is more compressed and the final value of x_{CO2} is reduced, the increase in porosity is smaller at higher pressure. For example, at a confining pressure of 100 MPa, ϕ increases from 0.0010 to 0.0029 (a factor of 2.9), at 150 MPa, ϕ increases by a factor of 1.3, and at 200 MPa, ϕ increases by a factor of only 1.1.

Other reactions affect the analysis primarily by the stoichiometric amounts of H_2O and CO_2 consumed and by the ΔV_{solid} of the reaction. An illustrative example is the reaction 3 anorthite + calcite + H_2O = 2 clinozoisite + CO_2, in which H_2O is replaced by CO_2 mole-for-mole. An increase in x_{CO2} at constant volume results in an increase in pressure, as shown in Fig. 3. The ΔV_{solid} for that reaction, though, is large enough to cause the pressure to drop with reaction progress. The relation between extent of reaction, as represented by the fluid composition, and pore pressure for the five reactions listed in Table 1 and for a confining pressure of 100 MPa is shown in Fig. 8. The relation between ξ and x_{CO2} is different for each reaction because of the different stoi-

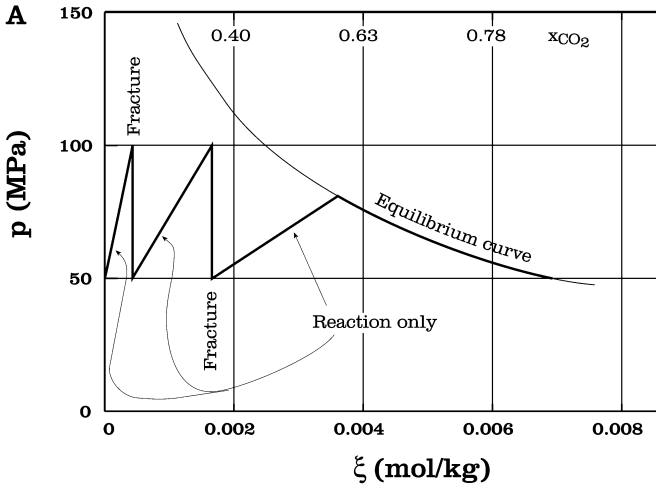

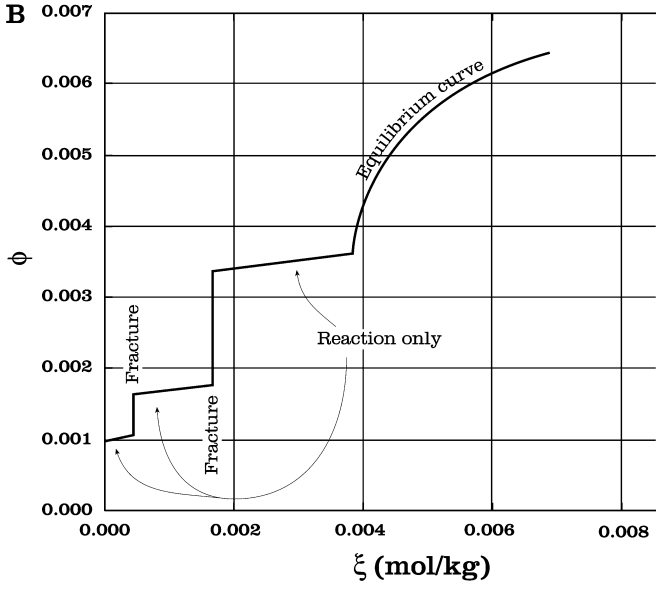

Fig. 6A, B Growth of cracks occurs once the pressure in the pores reaches the tensile strength. Cracks grow until the pore pressure drops to lithostatic pressure. **A** Fracture occurs twice before reaction changes the fluid composition sufficiently to reach the equilibrium composition. **B** Growth in crack volume resulting from reaction and fracture. Porosity grows from 0.1 to 0.6% until the fluid composition reaches the equilibrium value at lithostatic pressure

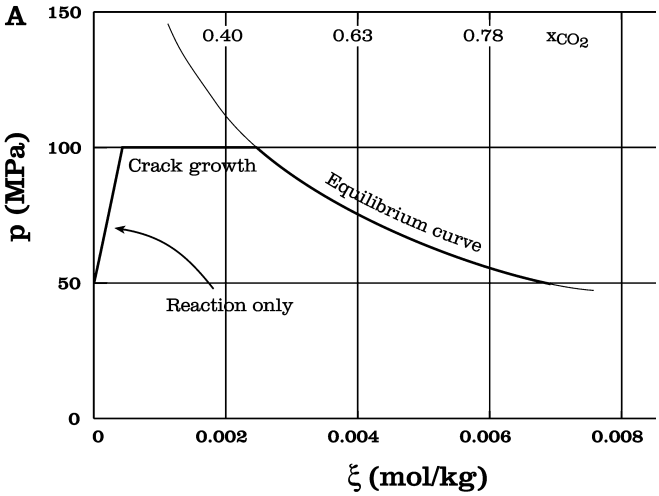

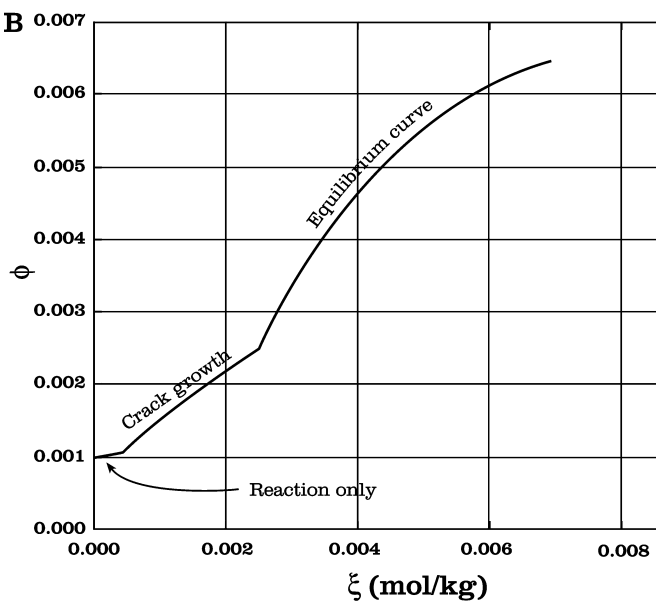

Fig. 7A, B Subcritical crack growth in which the fluid pressure remains at the threshold value as the crack grows. Once the equilibrium value is reached, crack growth is considered to continue until the fluid pressure drops to the lithostatic value. **A** Fluid pressure and **B** porosity as a function of reaction extent. The final pore volume and fluid composition are the same as in Fig. 6

chiometric values v_{CO2} and v_{H2O} for each. Each reaction also has a different ΔV_{solid}. In general, pressure increases to a maximum value, after which the continued increase in pore volume by reaction results in a decrease in pressure. Either the small equilibrium value of x_{CO2} or the limited strength of the rock prevents a great increase in pressure. In all cases, the extent of reaction required to reach the limiting pressure is $\leq \sim 5.0\times10^{-4}$ mol/kg.

Metamorphic rocks rarely have intergranular porosities on the order of 1%, so the pores and fractures collapsed or were filled with secondary minerals. Fracture porosity may also have formed along lithologic contacts. As long as fluid pressure was lithostatic or greater, though, the pores remained open. For a reaction such as reaction (6) in which the pore pressure drops, the porosity increase caused by ΔV_{solid} can be reduced if the pore volume collapses until the fluid pressure is lithostatic. Under that circumstance, the porosity increases because the molar volume of the fluid increases with increasing x_{CO2}, but the increase is less than that indicated by the loss in solid volume during reaction.

The analysis described here is a combination of the thermodynamic properties of fluid and of mineral equilibria with mass balance. Neither the rate of reaction nor that of fracture propagation is considered. The presumption is that the two are comparable and that reaction causes crack growth and vice versa. Laboratory measurements of the velocity of subcritical crack growth in marble and limestone are summarized by Atkinson

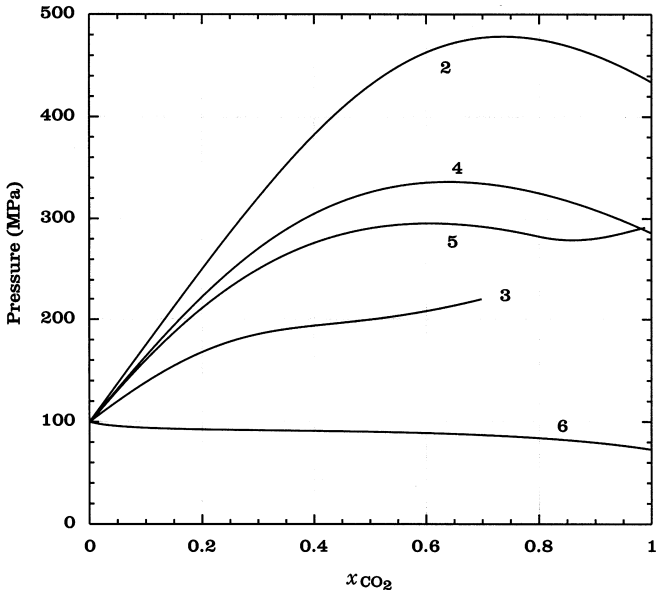

Fig. 8 Pore pressure as a function of reaction progress, expressed as fluid composition, for the reactions listed in Table 1. All reactions exceed the equilibrium values at 400 °C with only a small amount of reaction (compare Fig. 4). Only reaction (5) results in a pressure drop, which is a result of the large increase in pore volume from ΔV_{solid}

and Meredith (1987). Crack propagation rates are greater than 10^{-7} m/s for values of the stress intensity < 1.0 MPa $m^{1/2}$, which corresponds to a fracture length of ~0.2 mm for an effective pressure (p_f-p) of 50 MPa. For a crack growth rate of 10^{-7} m/s, the corresponding reaction rate ranges from 10^{-14} to 10^{-10} mol/s, depending on the shape of the crack. The required reaction rate is comparable with reaction rates measured in laboratory experiments (Kerrick et al. 1991), so the comparison is not unreasonable.

The model is based on the assumption of brittle failure, which for carbonate rock at 400 °C is not valid. If the rock behaves as a plastic, then at the yield strength, the rock deforms at a constant pressure, like the case shown in Fig. 7. If the rock undergoes strain hardening, then the pore pressure can increase to greater values than those suggested by the failure criterion.

In all the examples, pressure increases greatly to a limiting value with only small values of ξ; even at the equilibrium value of x_{CO2}, the value of ξ is generally $< 1.0\times10^{-2}$ kg^{-1}. That corresponds to a few tenths of a percent of the product assemblage in the mode. It is common to observe assemblages representing much greater values of ξ. For the example shown in Fig. 1, Labotka et al. (2000) determined that values of ξ were 10–20 times greater. Such large values of ξ in the example rock resulted from infiltration of fluid not in equilibrium with the rock and from reaction at the invariant point, both effective means of increasing the extent of reaction. The consequence of the high pressure generated by small values of ξ is rock fracture, which promotes open system behavior. Great values of ξ can then be achieved either by infiltration of an equilibrium fluid (Ferry and Dipple 1991), or by a combined infiltration–diffusion process similar to that described by Labotka et al. (1984).

Changes or gradients in pore fluid pressure are responsible for fluid flow and rock deformation. In aqueous fluids, pressure increases considerably with an increase in x_{CO2}, which is a common result of decarbonation reactions during metamorphism. At constant temperature, the magnitude of the effect of changing fluid composition on changing fluid pressure is second only to that produced by a change in the number of moles of fluid. In the case of closed pores, small extents of reaction create an overpressure sufficient to fracture carbonate rock and to promote open-system behavior.

Acknowledgements Research on the properties of metamorphic fluids has been supported in part by National Science Foundation grant EAR-0106990. Funding for J.G.B. was provided by the Division of Chemical Sciences, Geosciences, and Biosciences, Office of Basic Energy Sciences, US Department of Energy under contract DE-AC05-00OR22725, Oak Ridge National Laboratory, managed and operated by UT-Battelle, LLC. Sincere thanks go to B. Dutrow and an anonymous reviewer whose comments have greatly helped clarify the paper.

References

Atkinson BK (1987) Fracture mechanics of rock. Academic Press, London

Atkinson BK, Meredith PG (1987) The theory of subcritical crack growth with applications to minerals and rocks. In: Atkinson BK (ed) Fracture mechanics of rock. Academic Press, London, pp 111–166

Balashov VN, Yardley BWD (1998) Modeling metamorphic fluid flow with reaction–compaction-permeability feedbacks. Am J Sci 298:441–470

Blencoe JG, Seitz JC, Anovitz LM (1999) The H_2O–CO_2 system. II. Calculated thermodynamic mixing properties for 400 °C, 0–400 MPa. Geochim Cosmochim Acta 63:2393–2408

Dipple GM, Gerdes ML (1998) Reaction-infiltration feedback and hydrodynamics at the skarn front. In: Lentz DR (ed) Mineralized intrusion-related skarn systems. Mineralogical Society of Canada, pp 71–97

Domenico PA, Palciauskas VV (1979) Thermal expansion of fluids and fracture initiation in compacting sediments. Geol Soc Am Bull II 90:953–979

Duan Z, Møller N, Weare JH (1992) An equation of state for the CH_4–CO_2–H_2O system: II. mixtures from 50–1,000 °C and 0–1,000 bars. Geochim Cosmochim Acta 56:2619–2631

Dutrow B, Norton D (1995) Evolution of fluid pressure and fracture propagation during contact metamorphism. J Metamorph Geol 13:677–686

Ferry JM, Dipple GM (1991) Fluid flow, mineral reactions, and metasomatism. Geology 19:211–214

Holland TJB, Powell R (1990) An enlarged and updated internally consistent thermodynamic dataset with uncertainties and correlations: the system K_2O–Na_2O–CaO–MgO–MnO–FeO–Fe_2O_3–Al_2O_3–TiO_2–SiO_2–C–H_2–O_2. J Metamorph Geol 8:89–124

Holloway JR (1977) Fugacity and activity of molecular species in supercritical fluids. In: Fraser DG (ed) Thermodynamics in geology. Reidel, Dordrecht, pp 161–181

Jaeger JC, Cook NGW (1976) Fundamentals of rock mechanics. Chapman and Hall, London

Kerrick DM, Jacobs GK (1981) A modified Redlich–Kwong equation for H_2O, CO_2, and H_2O–CO_2 mixtures at elevated pressures and temperatures. Am J Sci 281:735–767

Kerrick DM, Lasaga AC, Raeburn SP (1991) Kinetics of heterogeneous reactions. Rev Mineral 26:583–671

Labotka TC (1992) Chemical and physical properties of fluids. Rev Mineral 26:13–42

Labotka TC, Souza PA (2002) Coupled isotope exchange and mineral reaction in the regionally metamorphosed dolomite rock, Death Valley, California. Am Mineral (in press)

Labotka TC, White CE, Papike JJ (1984) Evolution of water in the contact metamorphic aureole of the Duluth Complex, northeastern Minnesota. Geol Soc Am Bull 95:788–804

Labotka TC, Nabelek PI, Papike JJ (1988) Fluid infiltration through the Big Horse Limestone member in the Notch Peak contact metamorphic aureole, Utah. Am Mineral 73:1302–1324

Labotka TC, Souza P, Nabelek PI (2000) Coupled mineralogic reaction and isotopic exchange in regionally metamorphosed dolomite, Death Valley, California. Goldschmidt 2000. J Conf Abstr 5

Lockner DA (1995) Rock failure. In: Ahrens TJ (ed) Rock physics and phase relations. American Geophysical Union, Washington, DC, pp 127–147

Norton DL, Dutrow BL (2001) Complex behavior of magma-hydrothermal processes: role of supercritical fluid. Geochim Cosmochim Acta 65:4009–4017

Rice JM, Ferry JM (1982) Buffering, infiltration, and the control of intensive variables during metamorphism. In: Ferry JM (ed) Characterization of metamorphism through mineral equilibria. Mineral Soc Am, Rev Mineral pp 263–326

Seitz JC, Blencoe JG (1999) The H_2O–CO_2 system. I. Experimental determination of volumetric properties at 400 °C and 10–100 MPa. Geochim Cosmochim Acta 63:1559–1569

Span R, Wagner W (1996) A new equation of state for carbon dioxide covering the fluid region from the triple-point temperature to 1,100 K at pressures up to 800 MPa. J Phys Chem Ref Data 25:1509–1596

Sterner SM, Bodnar RJ (1991) Synthetic fluid inclusions. X: experimental determination of P–V–T–X properties in the CO_2–H_2O system to 6 kb and 700 °C. Am J Sci 291:1–54

Wagner W, Pruss A (1993) International equations for the saturation properties of ordinary water substance. Revised according to the international temperature scale of 1990. J Phys Chem Ref Data 22:783–788